Observations of aurorae by SPICAM ultraviolet spectrograph on board Mars Express: Simultaneous ASPERA-3 and MARSIS measurements

F. Leblanc,[1,2] O. Witasse,[3] J. Lilensten,[4] R. A. Frahm,[5] Ali Safaenili,[6] D. A. Brain,[7] J. Mouginot,[4] H. Nilsson,[8] Y. Futaana,[8] J. Halekas,[7] M. Holmström,[8] J. L. Bertaux,[1] J. D. Winningham,[5] W. Kofman,[4] and R. Lundin[8]

Received 16 January 2008; revised 12 May 2008; accepted 4 June 2008; published 22 August 2008.

[1] We present a new set of observations of Martian aurorae obtained by Spectroscopy for the Investigation of the Characteristics of the Atmosphere of Mars (SPICAM) on board Mars Express (MEX). Using nadir viewing, several auroral events have been identified on the Martian nightside, all near regions of crustal magnetic fields. For most of these events, two to three consecutive events with variable intensities and separated by a few seconds to several tens of seconds have been observed, whereas simultaneous observations with Mars Advanced Radar for Subsurface and Ionosphere Sounding (MARSIS) and Analyzer of Space Plasma and Energetic Atoms (ASPERA-3) have been possible. In this paper, we present the data set for these events and discuss the possible correlation between the measured UV emission by SPICAM, the measured downward and/or upward flux of electrons by ASPERA-3 and the total electron content recorded by MARSIS. Despite the limited coverage of SPICAM ultraviolet spectrograph (UVS) on the Martian nightside (essentially in regions of high crustal magnetic fields), there is however a very good correlation between the regions with the locally smallest probability to be on closed crustal magnetic field lines, as derived from Mars Global Surveyor/Electron Reflectometer (MGS/MAG-ER), and the position of an aurora event. This suggests that the crustal magnetic fields, when organized into cusp-like structure, can trigger the few aurorae identified by SPICAM UVS. It confirms also the good probability, in the cases where SPICAM UVS measured UV emissions, that the increase in the measured total electron content by MARSIS and the simultaneous measured precipitating electron flux by the ASPERA-3/Electron Spectrometer may be related to each other.

Citation: Leblanc, F., et al. (2008), Observations of aurorae by SPICAM ultraviolet spectrograph on board Mars Express: Simultaneous ASPERA-3 and MARSIS measurements, *J. Geophys. Res.*, *113*, A08311, doi:10.1029/2008JA013033.

1. Introduction

[2] After 1 decade of observations of magnetic fields and electrons near Mars, the Magnetometer and Electron Reflectometer (MAG-ER) on board Mars Global Surveyor (MGS) has completely changed our view of Mars' plasma environment [*Nagy et al.*, 2004]. The discovery of strong crustal magnetic field structures revealed the existence of a past Martian dynamo [*Acuña et al.*, 2001] and strongly affected our understanding of the past history of Mars' atmosphere [*Chassefière et al.*, 2006]. The long-term observation of these magnetic structures has also demonstrated their present influence on Mars' interaction with the solar wind [*Nagy et al.*, 2004]. In particular, electron spike events have been observed in relation to maxima of the crustal magnetic field radial component [*Mitchell et al.*, 2001]. At 400 km, electron flux spikes have been identified as an electron energy distribution of magnetosheath type, measured during short periods (down to 8 s), and usually observed between two plasma voids (defined as regions in which the measured electron flux is below the noise level of MAG-ER/MGS). *Mitchell et al.* [2001] interpreted these measurements as the evidence of a past or present reconnection of the crustal magnetic field lines to the interplanetary magnetic field lines. *Mitchell et al.* [2001] also pointed out the analogy between such a magnetic field structure and Earth's magnetospheric cusp. In the same way as in the Earth's auroral cusps, in region of strong crustal magnetic fields, particles may precipitate into Mars' atmosphere and/or escape from it. This

[1]Service d'Aéronomie, CNRS, IPSL, Verrières-le-Buisson, France.
[2]Currently at Osservatorio Astronomico di Trieste, Trieste, Italy.
[3]Research and Scientific Support Department, ESA, ESTEC, Noordwijk, Netherlands.
[4]Laboratoire de Planétologie de Grenoble, Grenoble, France.
[5]Southwest Research Institute, San Antonio, Texas, USA.
[6]Jet Propulsion Laboratory, Pasadena, California, USA.
[7]Space Sciences Laboratory, University of California, Berkeley, California, USA.
[8]Swedish Institute of Space Physics, Kiruna, Sweden.

Copyright 2008 by the American Geophysical Union.
0148-0227/08/2008JA013033

conclusion has been recently confirmed by Analyzer of Space Plasma and Energetic Atoms (ASPERA-3) on board Mars Express (MEX) by *Lundin et al.* [2006] as well as by MAG-ER/MGS [*Brain et al.*, 2006]. In particular, *Lundin et al.* [2006] observed downward energetic electron fluxes with typical terrestrial auroral-type energy distributions in association with energetic upflowing ion fluxes. This points to possible processes of acceleration or heating between the Martian ionosphere and the Martian magnetosheath and magnetotail [*Dubinin et al.*, 2008a].

[3] A downward flux of energetic particles can also lead to auroral emissions of the type observed by Spectroscopy for the Investigation of the Characteristics of the Atmosphere of Mars ultraviolet spectrograph (SPICAM UVS) on Mars Express [*Bertaux et al.*, 2006]. The only observation published so far of such an emission was clearly associated with the strongest crustal magnetic field structure [*Bertaux et al.*, 2005]. This observation has also been recently reanalyzed and has been shown to be most probably produced by primary electrons of few tens eV energy [*Leblanc et al.*, 2006b]. Therefore, either these electrons have been transported from the Martian dayside ionosphere [*Dubinin et al.*, 2008b] or they are nonaccelerated magnetosheath electrons as observed in nightside crustal magnetic field regions by *Mitchell et al.* [2001] and *Liehmon et al.* [2003]. Actually, a recent analysis based on a 3-D magnetohydrodynamic approach of the magnetic field draping around Mars suggested that the most likely electrons which produced the observed UV aurora emission were nonaccelerated magnetosheath electrons rather than photoelectrons [*Liehmon et al.*, 2007].

[4] A downward flux of particles may also locally ionize the Martian atmosphere and may lead to a local increase of the ionospheric electron content. This has been recently observed by *Safaeinili et al.* [2007] using Mars Advanced Radar for Subsurface and Ionosphere Sounding (MARSIS) on board Mars Express. These authors found a significant correlation between the maxima of the total electron content (that is the total number of electrons between Mars Express and the surface in a column density) as measured by MARSIS on the nightside and the presence of a strong radial crustal magnetic field component.

[5] In this paper, we present nine new auroral-type emission events identified within the SPICAM UV observations on the Martian nightside (section 2). Eight of these events have been measured when two other Mars Express instruments were operating: ASPERA-3 and the MARSIS radar sounder. The possible correlation between SPICAM UV observation, ASPERA-3 particle measurements and MARSIS total electron content is therefore discussed in section 3.

2. SPICAM UVS Observations

[6] SPICAM UV spectrograph is part of the SPICAM instrument (also composed of an IR spectrograph covering 1.1 and 1.7 μm) which is dedicated to solar occultation and nadir viewing observations. SPICAM UV spectrograph has a 118–305 nm wavelength range with a 1.5 nm spectral resolution for the light passing through the narrow part of SPICAM slit and a 6 nm spectral resolution with a $\sim$8 times larger sensitivity for the light passing through the large part of the slit [*Bertaux et al.*, 2006]. During each observation by SPICAM UVS, five spatially adjacent parts (that we will call spatial bin) of the CCD are recorded leading to five individual spectra each second (the time for one integration lasting $\sim$0.6 s and a complete reading of these five lines of the CCD, $\sim$0.4 s). Typically, one to two thousands times five individual spectra are recorded during the 20 to 30 min of an observation. Of these five spatial bins, two have been obtained with the best spectral resolution (spatial bins numbered 0 and 1) and two with the worst spectral resolution (spatial bins numbered 3 and 4). The spatial bin numbered 2 cannot be used because it measured light with both spectral resolutions and cannot be properly calibrated. The procedure to subtract offset and nonuniform dark current and to integrate the spectral emission have been described in detail by *Leblanc et al.* [2006a] and will not be repeated here. The geometry of each observation, its UT time, and the solar conditions are given in Table 1.

[7] Following the first observation of an auroral-type emission event in the Martian atmosphere by the SPICAM UVS [*Bertaux et al.*, 2006; *Leblanc et al.*, 2006b], several dedicated observations have been made during periods when the periapsis of Mars Express was on the nightside. Nadir mode viewing has been preferentially selected in order to map the position where these aurorae occur and to obtain coordinated observations with other instruments on board Mars Express. We added two limb viewing observations in Table 1, one during the first identified event recorded during orbit 716 [*Bertaux et al.*, 2005; *Leblanc et al.*, 2006b] and the second during orbit 2800. However, we will not discuss them in this paper. An auroral event is identified when we observe a significant increase of the signal (by more than two standard deviations with respect to the mean signal) simultaneously on (1) the two spatial bins facing the large slit (highest sensitivity) and (2) on the total measured signal (summed over the five spatial bins). In order to avoid the parts of the spectra with low signal/noise ratio we have only considered a spectral region between 150 and 280 nm excluding the edges of the spectral range. The increase must last more than two consecutive integrations in order to be validated. We have tested observations from 66 nightside passes of MEX and found only six orbits with auroral events. It is difficult to deduce from this set of observations any significant statistics since from these 66 cases, only nine limb viewing orbits were obtained when the spacecraft was below 320 km and 21 nadir viewing orbits had a portion below 1000 km. This limit in altitude is imposed by the sensitivity of SPICAM UVS which constrains its capability to detect faint aurora emissions occurring below 200 km in altitude.

[8] Because these observations have been performed with nadir viewing, the typical intensity observed for the main auroral emissions is significantly smaller than during limb viewing as a result of the different path lengths through the region of the emission. This difference is typically of the order of a factor 13 for dayglow observations following *Leblanc et al.* [2006a]. The method used to extract the auroral emission intensities (subtraction of a background associated with the nightglow emission and integration of the emission lines) has been described by *Bertaux et al.* [2005] and *Leblanc et al.* [2006b]. For most observations it has been possible to identify the Cameron band system emission [*Leblanc et al.*, 2006a, b]. The Cameron band

Table 1. Set of Auroral Emission Events[a]

Date MEX Orbit	Ls (°)	F10.7	SW Conditions	SPICAM Viewing	Time Period (UT)	S/C Altitude (km)	Aurora Longitude (°)	Aurora Latitude (°)	Cameron Band Emission (R)	Emission at 289 nm (R)
2004 07 07 591	57.1	54.1	SEP event high SW pressure southward IMF	nadir	0539:52–0539.55	670	214	34S	241 ± 50	N/A
									105 ± 10	N/A
					0541:17–0541:36	586	214	39S	218 ± 34	N/A
									195 ± 10	13 ± 8
2004 08 11 716	72.4	39.4	dawnward - southward IMF	limb	0601:21–0601:28	266	178	50S	2040 ± 132	126 ± 56
									1546 ± 41	157 ± 26
2005 12 27 2515	347.3	38.3	no SEP event moderate to high SW pressure southward IMF	nadir	2147:31–2147:41	954	158	41S	341 ± 74	146 ± 70
									175 ± 16	50 ± 26
					2151:08–2151:16	700	158	52S	588 ± 90	N/A.
									662 ± 24	120 ± 30
2006 01 26 2621	2.4	32.7	no SEP event moderate SW pressure dawnward IMF	nadir	1404:01–1404:15	564	182	40S	414 ± 61	N/A
									274 ± 14	34 ± 15
2006 02 19 2705	13.9	30.0	no SEP event moderate to high SW pressure dawnward–southward IMF	nadir	0237:56–0238:11	387	206	40S	187 ± 36	N/A.
									105 ± 9	27 ± 11
					0238:34–0238:48	365	206	42S	663 ± 51	57 ± 37
									547 ± 16	94 ± 15
					0240:52–0241:02	309	206	52S	273 ± 46	31 ± 30
									214 ± 11	12 ± 8
2006 03 17 2800	25.5	29.3	southward IMF	limb	1709:46–1710:16	314	237	31S	597 ± 41	35 ± 16
									826 ± 17	164 ± 13

[a]Two values of the Cameron band emission and of the 289 nm emission are given for each event. The first value has been derived from the average spectrum of the two spatial bins with the best spectral resolution and the second value using the spatial bins with the worst spectral resolution. Each spatial bin covered 32 pixel rows of the CCD. F10.7 (10^{-22} W/m^2/Hz) values are calculated from daily average National Geophysics Data Center taking into account the relative positions of the Earth and Mars, the Sun rotation, and Mars' heliocentric distance. N/A indicates that the emission intensity cannot be estimated better than one sigma uncertainty. SW conditions: Solar wind conditions as inferred from low altitudes dayside measurement of the magnetic pressure by MGS/MAG-ER [*Crider et al.*, 2003]. SEP is for solar energetic particles [*Brain et al.*, 2006]. IMF direction is accurate at ~90°. S/C is for MEX spacecraft.

emission ($a^3\Pi - X^1\Sigma^+$) from 180 to 260 nm is the most intense emission measured in Mars' dayglow [*Barth et al.*, 1971; *Leblanc et al.*, 2006a] and is thought to be produced by the photo and electron-impact dissociation of the CO_2 atmospheric molecules leading to CO molecule in $a^3\Pi$ excited state. On the Martian dayside, a typical intensity of a few tens of kilorayleigh (kR) has been measured by SPICAM UVS [*Leblanc et al.*, 2006a]. In some cases, it has been possible to extract the 289 nm emission which corresponds to the CO_2^+ ultraviolet doublet ($B^2\Sigma^+ - X^2\Pi$) emission. Typically, the CO_2^+ emission's intensity is 10 kR on the dayside. It is produced by photon and electron-impact ionization of the atmospheric CO_2 molecule leading to the excited state CO_2^+ ($B^2\Sigma^+$). Figure 1 displays an example of auroral spectra measured during orbit 2621. These spectra are noisy with respect to dayglow measurements [*Leblanc et al.*, 2006a] because they are the average of only 28 individual spectra with respect to the 1000 individual spectra used on the dayside. However, in both Figures 1a and 1b, it is possible to clearly identify the main features of the Cameron band system using both types of spectral resolution and also to identify the 289 nm emission in Figure 1b which corresponds to the spatial bin with the lowest spectral resolution but the highest sensitivity. In the aurora spectra, no emissions like the bright dayglow O 130.4 nm emission, Lyman α H 121.6 nm emission, or the CO fourth positive emission [*Leblanc et al.*, 2006a] can be identified. However, the dayside O 130.4 nm and Lyman α H 121.6 nm emissions are essentially produced by resonant scattering of solar photons. Moreover, the CO fourth positive $A^1\Pi - X^1\ \Sigma^+$ emission was present in the aurora spectrum published by *Bertaux et al.* [2005] but because it has a weak spectral signature, its signal/noise ratio is probably too small when measured with SPICAM's nadir field-of-view orientation.

[9] Another difficulty in the identification of the auroral emission has been introduced by the nonnominal behavior of SPICAM UVS during the extended mission of Mars Express. Such behavior is characterized by the sudden increase or decrease during a few seconds of the measured signal on the used and masked pixels (that are pixels which are physically masked from the light and measured only the dark current of the CCD [see *Bertaux et al.*, 2006]). Figure 2 displays an example of such a behavior. As shown in Figure 2a, the signal measured on the masked pixel during the whole sequence of observation of orbit 2621 evolved smoothly showing the typical and nominal variation of the dark current. In contrast, Figure 2b displays the masked signal measured during orbit 2705. As shown, frequent short time variations of the masked signal are observed most of the time before 0234:04 and around 0235:33 and 0237:01. After 0237:20 up to the end of the sequence of observation, the masked signal is almost clear of any event. In the present work, we have considered the period after 0237:20 as nominal using the masked signal as an indicator of any nonnominal behavior. Three aurora events have been identified during orbit 2705 and are all clearly not associated with short-term intense variations of the masked signal.

[10] Figure 3 displays the trajectories of Mars Express during all the nadir viewing observations made when the spacecraft was below 1000 km altitude. These trajectories have been plotted on a map of the radial component of the crustal magnetic field as calculated at 200 km altitude by *Purucker et al.* [2000]. The white crosses represent the positions where the observations of auroral-type event occurred. As shown in Figure 3, all auroral events occurred

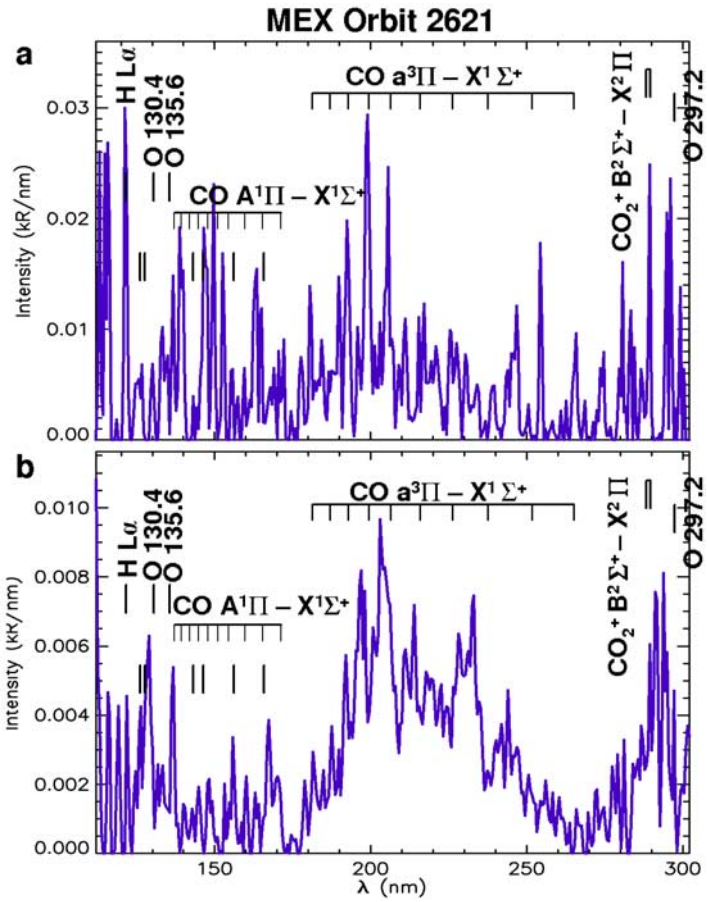


Figure 1. SPICAM ultraviolet spectrograph (UVS) spectra of the aurora event during orbit 2621. (a) As measured with the spatial bins facing the narrow part of the slit (best spectral resolution) during 14 s. (b) As measured with the spatial bins facing the large part of the slit (lowest spectral resolution). Each spectrum is the average of the 28 individual spectra measured during this event on the two spatial bins (14 each) either with the worst spectral resolution or the best one.

in the region of strongest crustal magnetic field (in the Southern Hemisphere centered on a region at 180° in longitude). Actually, during several trajectories over these magnetic structures no observation of auroral events occurred. No auroral events were observed southward of 60° in latitude, even though the spacecraft was below 1000 km altitude at high southern latitudes for some of these passes. There is also no obvious correlation between emission intensity and local time of the auroral event. All observations performed during these 21 orbits have been obtained between 18 h local time and 22 h local time, and the auroral events are uniformly distributed within this local time range. There is no obvious correlation between these observations and the occurrence of solar energetic particle events as inferred from the MGS/MAG-ER data set (Table 1).

3. Simultaneous Measurements by Other Instruments

3.1. ASPERA-3/MEX, MARSIS/MEX, and MAG-ER/MGS Instruments

[11] The main advantages of nadir viewing observations are the accurate location of the aurora on a magnetic field map (Figure 3) and the opportunity to obtain coordinated observations with other instruments on board Mars Express, in particular with ASPERA-3 and MARSIS. ASPERA-3 is composed of two energetic neutral analyzer detectors (Neutral Particle Imager, NPI, and Neutral Particle Detector, NPD), an electron spectrometer (ELS) and an ion mass analyzer (IMA) [*Lundin and Barabash*, 2004]. During the set of observations described in the previous section, only ELS and IMA were operating. The ELS is made up of a collimator followed by a standard spherical top hat electrostatic analyzer with a microchannel plate and anode ring to count electrons. ELS can measure the electron energy distribution within a 360° × 4° field of view (with 16 sectors each of 22.5° × 4°). The energy range is from 0.9 eV to 20 keV with an energy resolution of 8%. A complete energy sweep is performed every 4 s [*Winningham et al.*, 2006]. The IMA energy range is between 0.01 and 30 keV/q with a 5.6° × 360° field of view and a capability of electrostatic sweeping to cover the elevation angle of ±45° in 16 sectors. IMA is a spherical electrostatic analyzer followed by a circular magnetic separation section and a circular microchannel plate imager providing the mass and azimuth of the incident particle. A full 3-D spectrum accumulation sweep of 16 polar angles × 16 azimuthal sectors × 32 mass rings × 96 energies requires 192 s to complete, whereas a 16 azimuthal sectors × 32 mass rings × 96 energies requires 12 s [*Carlsson et al.*, 2006]. ELS is located on a scanning platform which is placed

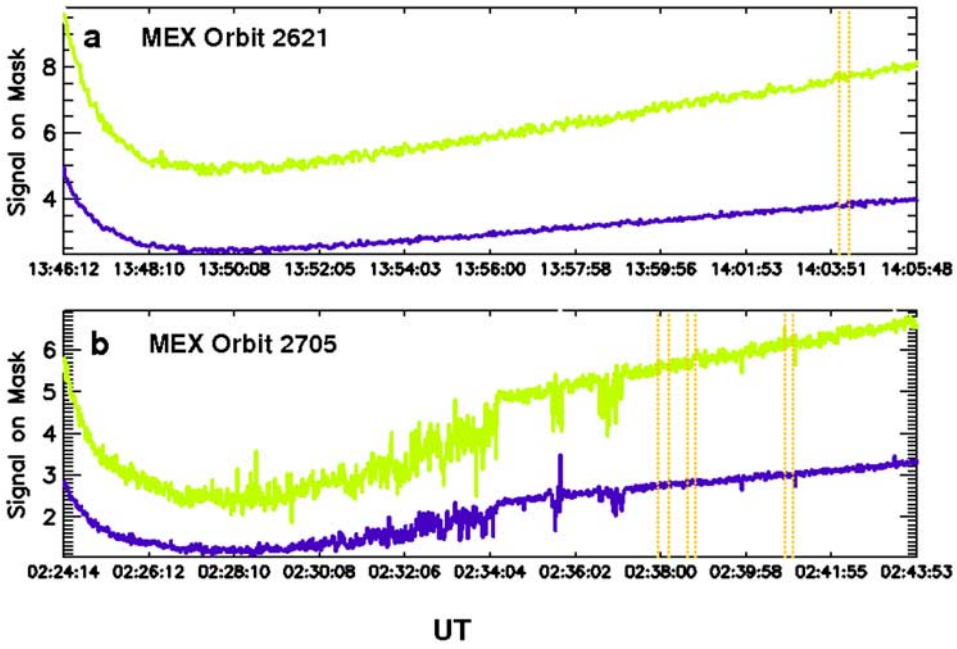


Figure 2. SPICAM UVS measurements of the masked signal during (a) orbit 2621 and (b) orbit 2705. The gray solid line corresponds to the signal measured on the spatial bin numbered 4 (worst spectral resolution), whereas the dark solid line corresponds to the masked signal measured on the spatial bin numbered 0 (best spectral resolution). The dark solid line was shifted by a factor 0.5 for clarity. The dotted vertical lines correspond to the period(s) during which an aurora event has been spectrally identified.

at the edge of a side of the spacecraft where the SPICAM UVS has been mounted (that is the nadir facing side of the spacecraft during the observations discussed here). IMA has been placed at the edge of the opposite side of the spacecraft. As a consequence, in the particular case of SPICAM UVS nadir pointing, part of the field of view of ELS will be covered by the spacecraft when looking for precipitating electrons and IMA will have its field of view covered partly by the spacecraft when looking for outflowing flux.

[12] MARSIS was deployed on MEX in May–June 2005. It is a multifrequency synthetic aperture orbital sounding radar which operates below 800 km and can be used either to sound the ionospheric plasma (Active Ionosphere Sounder mode, AIS) or to sound the subsurface with frequency

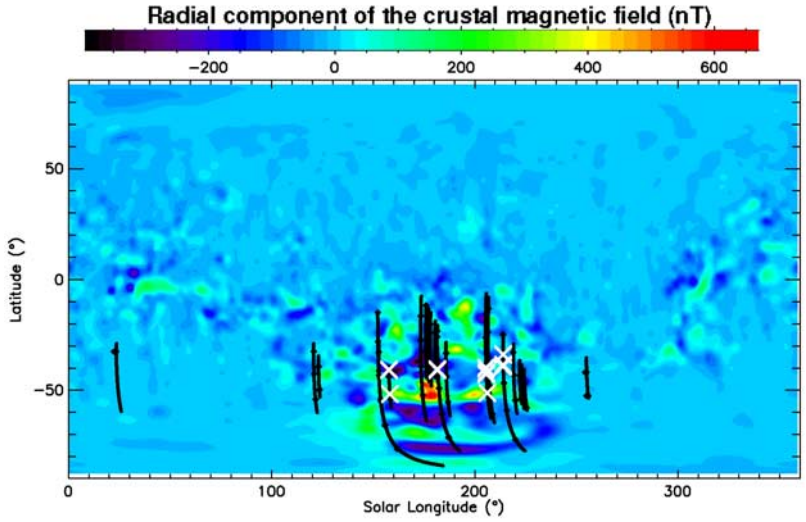


Figure 3. Trajectories of Mars Express during nadir viewing observations by SPICAM UVS. Only the part of each orbit with the spacecraft below 1000 km in altitude has been plotted. These trajectories are plotted on a 2-D map of the radial component of the Martian magnetic crustal field as calculated at 200 km in altitude [*Purucker et al.*, 2000]. The positions of the identified aurora during these nadir viewing orbits are also plotted with white crosses.

between 1.3 and 5.5 Mhz [*Picardi et al.*, 2004]. To sound the subsurface, the signal frequency must be larger than the maximum plasma frequency. In that case, the ionosphere will still disperse the signal phase. The ionospheric phase distortion may then be analyzed to retrieve the total electron content (TEC) of Mars' atmosphere between the altitude spacecraft and the surface [*Mouginot et al.*, 2008]. Such distortion has been intensively analyzed for 750 MEX orbits during their nightside operation and successfully correlated with Mars' crustal magnetic fields [*Safaeinili et al.*, 2007]. *Safaeinili et al.* [2007] found a high concentration of high value of the TEC in regions of high intensity of the crustal radial magnetic field as measured by MGS/MAG-ER. The lateral spatial resolution of MARSIS in subsurface sounding mode is 10 to 30 km in the cross-track direction, the along-track footprint resolution being between 5 and 10 km. A TEC is calculated every 2 s [*Mouginot et al.*, 2008].

[13] On board Mars Global Surveyor, the Electron Reflectometer (ER) and Magnetometer (MAG) instruments were also operating [*Mitchell et al.*, 2001]. The ER instrument consists of a hemispherical imaging electrostatic analyzer followed by a microchannel plate and a resistive imaging anode. An integration lasts between 2 to 48 s. The field of view is $360^\circ \times 14^\circ$ with $22.5^\circ \times 14^\circ$ angular resolution. The energy range is between 10 eV to 20 keV with an energy resolution of 25%. The count rate is accurate within a 10% uncertainty. The MAG instrument provides fast vector measurement (up to 32 samples/s) of the Martian magnetic field and is composed of two redundant triaxial magnetometers. MGS was on a circular orbit at 405 ± 36 km at a fixed local time of 0200/1400 (period of rotation of 1.96 h) during its orbital mapping phase at the time of the present discussed measurements.

3.2. ASPERA-3/MEX, MARSIS/MEX, and MAG-ER/MGS Measurements

[14] Figure 4 displays the different measurements obtained by SPICAM UVS (Figure 4g), MGS/ER (Figure 4f), ASPERA-3/ELS (Figures 4d and 4e), MARSIS (Figure 4c), and the Mars Express altitude (Figure 4a) and latitude (Figure 4b). The track of Mars Express during this orbit was at a local time of 2030 at a longitude of 180° that is above the most intense crustal magnetic field recorded by MGS/MAG. Between 1404:01 and 1404:15 (between the two dotted vertical lines of Figure 4), SPICAM UVS observed a significant increase of the total observed light (Figure 4g). The corresponding spectra measured during this period are displayed (Figure 1) and are clearly composed of the main Cameron band emission features highlighting the occurrence of an auroral event. During the same period (within the 4-s time resolution of ELS), ASPERA-3/ELS measured an increase of the total energy flux (Figure 4e), by one order of magnitude followed by a decrease of this flux by two orders of magnitude. The electron energy distribution is displayed in Figure 5. We only display the signal measured in sectors 1 to 11 of ASPERA-3/ELS which cover a total field of view of $247.5^\circ \times 4^\circ$, because sectors 0, 12, 13, 14, and 15 are partially facing the spacecraft. The energy distribution of Figures 4 and 5 is an isotropic electron distribution exhibiting an atmospheric loss cone with a peak in flux at an energy of 80 eV for all sectors numbered 1 to 11; the exception being sectors 6 and 7. During this orbit, the nadir direction lies between sectors 7 and 8. Therefore sectors 1, 2, and 3 measured downward electron fluxes along the radial direction. Sectors 4 and 5 measured electrons perpendicularly to the radial direction, whereas sectors 6 and 7 and sectors 8 and 9 cover angles between 0° and 45° from the nadir direction. Since ASPERA-3/ELS observations have been made above a strong region of radial crustal magnetic field, it is possible to use the *Cain et al.* [2003] model of the crustal magnetic field to infer the electron pitch angle distribution with respect to the sectors of ASPERA-3/ELS. This model suggests that sectors 1, 2, and 3 measured electrons with pitch angle between 40° and 96°, sectors 4 and 5 between 114° and 131°, sectors 6 and 7 to 155°, and sectors 8 and 9 between 120° and 130°. The angular distribution displayed in Figure 5 may therefore be interpreted as an isotropic electron distribution which is channeled into the atmosphere by the crustal magnetic field lines, interacting with the atmosphere by loosing energy which is going into the generation of the auroral signatures, that is a loss cone electron distribution already reported as associated to Martian aurorae [*Brain et al.*, 2006].

[15] ASPERA-3/IMA did not measure any ion flux during this event (and actually during none of the auroral events identified by SPICAM UVS). It is most probably due to the fact that IMA is mounted on the opposite side of the spacecraft facing the zenith, so that an ion beam coming from below the spacecraft might be partially blocked by the spacecraft. When IMA is in electrostatic scanning mode, the field of view partially covers the nadir direction but only 1/16 of the time, the scanning lasting 192 s (case of orbits 591, 2621, and 2705). For the case with no electrostatic scanning with a 12-s resolution (orbit 2515), IMA should be able to observe ions passing through the spacecraft, unless the path is blocked by the solar panel. Unfortunately, the nadir direction is between two sectors where the sensitivity of IMA is much lower. Therefore, a beam along the nadir direction must have a certain angular width to be observed, at least more than about 10°. According to *Lundin et al.* [2006], the typical ionospheric ions accelerated by a field-aligned electric field observed by ASPERA-3/IMA can have a very narrow angular width so that IMA is rather unlikely to observe these ion beams when SPICAM UVS is pointed toward the nadir direction.

[16] Figure 4c provides the total electron content as deduced from MARSIS subsurface sounding mode during orbit 2621. There is a clear peak of the TEC during the time of SPICAM UVS measurement of an auroral event. It is also interesting to notice that the TEC variation is much broader than in the case of ASPERA-3/ELS or SPICAM/UVS measurements. This broadening is larger than MARSIS spatial/temporal resolution so that it suggests a much larger region of increased electron density along the track of MARSIS. A second peak of the TEC just before the one corresponding to the auroral event can also be seen in Figure 4c (just before 1403:43). Examination of the ASPERA-3 measurement at that time shows a spike of electron flux. Moreover, a small increase of the signal has also been measured by SPICAM UVS during that period (Figure 4g) but is not significant enough to be identified as an auroral event according to our criteria.

[17] During orbit 2621, MGS was on the nightside at 240° longitude in the same range of latitude as MEX. The

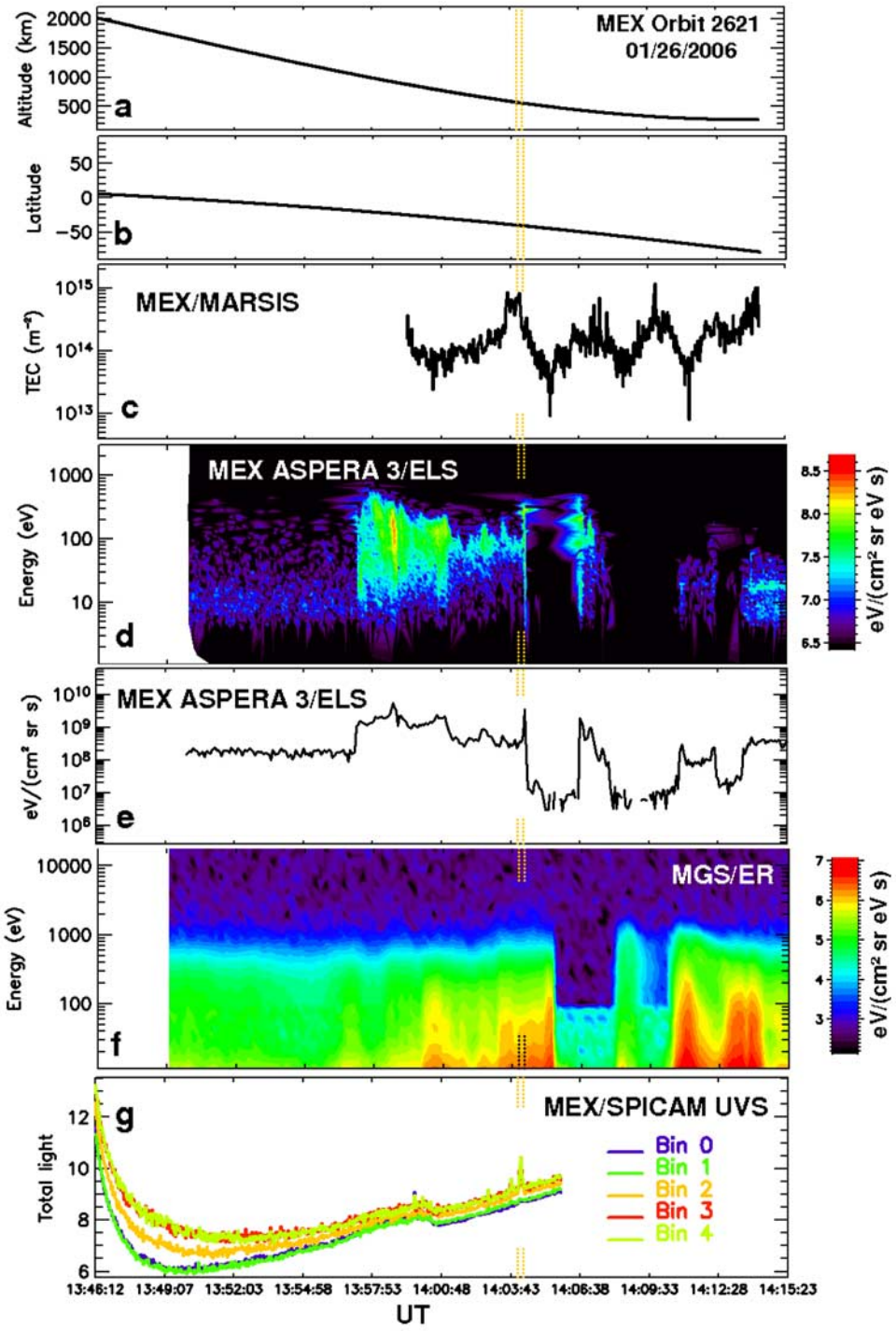


Figure 4. Time series of the measurements during orbit 2621. Shown is the MEX (a) altitude and (b) latitude, (c) MEX/MARSIS Total Electron Content, (d) MEX/ASPERA-3/ELS sector 1 (which is the sector facing the zenith) electron measurement in eV/(cm^2 ster eV s), (e) MEX/ASPERA-3/ELS energy flux of sector 1, (f) MGS/MAG-ER electron energy flux averaged over the full set of sectors in eV/(cm^2 ster eV s), and (g) MEX/SPICAM UVS measurements summed over the full spectral range for each spatial bin in ADU. Indicated on each by vertical dotted lines are the periods during which an aurora event has been identified in SPICAM UV observations.

electron energy spectrum is tail-like, and there may be some hints of photoelectrons at 40 eV and near 500 eV. MGS was passing from a region of field lines unconnected to crustal magnetic fields into a region of open and closed crustal field lines. At the moment of the auroral event, the electron energy distribution measured by MGS/ER is isotropic over the range of pitch angles sampled by MGS/ER. It usually indicates closed magnetic field lines [*Brain et al.*, 2007].

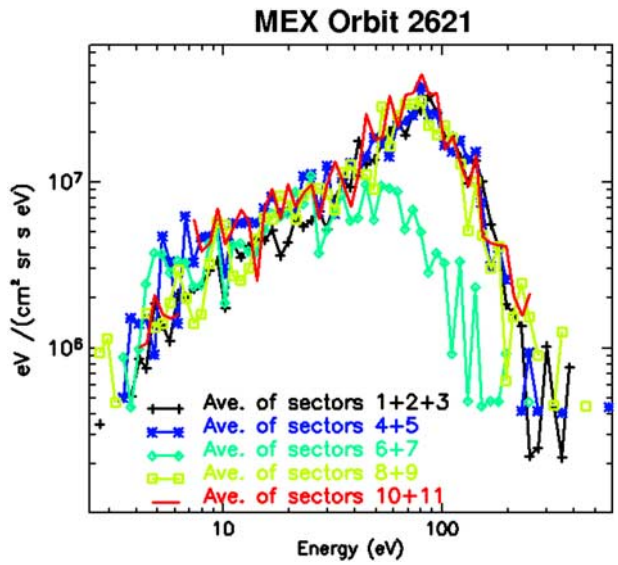


Figure 5. Electron differential energy flux measured by MEX/ASPERA-3/ELS during orbit 2621 between 1404:01 and 1404:15. In order to improve the figure, measurements in adjacent ELS sectors displaying a similar energy distribution have been averaged. Sectors 1 and 9 are 180° apart. No correction of the spacecraft potential has been done. Typical potentials between −4.5 and −5.5 V are estimated from the energy position of the photoelectron peaks during nearby time periods.

[18] In Figure 6, we display the same information as in Figure 4 but during orbit 2705. From the beginning of SPICAM measurements up to 0236 UT a typical non-nominal behavior of the instrument is seen (also seen in Figure 2b). It is followed by a nominal period that follows our criteria (see section 3.1). The dotted vertical lines indicate the times of auroral emissions observed by SPICAM UVS based on spectral identification. Mars Express was at less than 400 km in altitude during the auroral emissions. Figure 6 clearly shows a good temporal correlation (considering the time resolution of each instrument) between SPICAM aurora emissions (Figure 6f), downward electrons measured by ASPERA-3 (Figure 6d, sector 1 facing the zenith direction) and a significant increase of the Total Electron Content of the Martian ionosphere (by a factor 5, 6, and 3 with respect to the background signal in cases 2705a, 2705b, and 2705c, respectively, as displayed in Figure 6c). During this period, MGS was on the dayside passing over the fringes of a crustal magnetic field region near the North Pole. MGS did not show any high instrument background (no solar event) but recorded a dawnward IMF and a normal solar pressure. The measurements during orbit 2705 are particularly interesting since the SPICAM UV spectrograph observed two events, 2705a and 2705b, separated by 40 s (that is by approximately 200 km apart) whereas ASPERA-3 (in the 4-s time resolution mode) observed at 387 and 362 km an almost continuous downward flux of electron with similar energy distributions (see Figures 6d and 6e). At the time of the SPICAM UV observations (2705a and 2705b cases), Mars Express was above a crustal magnetic field anomaly with a 200–400 nT radial component at 200 km in altitude. Following the *Cain et al.* [2003] model of the crustal magnetic field, the sector 1 displayed Figure 6d measured electrons with pitch angle around 60° during events 2705a and 2705b, whereas this sector 1 measured electrons with pitch angle around 150° during event 2705c. In another way, from events 2705a and 2705b to event 2705c Mars Express crossed radial crustal magnetic field lines upward for the two first events and downward for event 2705c. The TEC derived from MARSIS measurements displays a somewhat similar configuration than that of orbit 2621. Two peaks in the TEC are observed almost simultaneously to SPICAM UVS auroral emission observations. These two peaks are seen in the MARSIS data at the top of a much broader peak centered between the two SPICAM UV aurora emissions, suggesting that MARSIS observed an extended region of large electron content.

3.3. Potential Correlation Between SPICAM UVS, ASPERA-3/ELS, and MARSIS

[19] In Table 2, we summarized the different parameters measured during each auroral event identified by SPICAM UVS with a nadir viewing. There is no obvious relation between impacting energy flux as measured by ASPERA-3/ELS and the observed Cameron band and 289 nm doublet emission intensities. However, the brightest Cameron band emission is associated with the largest incident energy flux (case 2515b). The other cases, namely 591a and b, 2515a, 2621, and 2705a, b, and c, do not show any particular relation between intensity of the incident electron flux and intensity of the emissions. This can be due to the variable altitude of the spacecraft (as an example in the case of 2515a the spacecraft was at an altitude of 940 km). The spacecraft potential may also have changed significantly the incident electron flux, particularly for the electron distribution peaking at low energy (591b, 2621a, and 2705c). Moreover, the total zenith observed emission is in a large part produced by secondary electrons of lower energy. This is particularly true for the Cameron band emission since its cross section peaks around 80 eV [*Avakyan et al.*, 1998]. The production of this secondary electron as well as their altitude of production depends significantly on the initial distribution in energy of the incident electrons. It is therefore not surprising to find a significant difference between cases 2621a and 2705a as an example and to a lesser extent between cases 2705a and 2705b where electron energy distributions as measured by ASPERA-3/ELS significantly differ from one another. Moreover, the transport of primary and secondary electrons within the Martian atmosphere, key parameter in constraining the integrated emission, will depend significantly on the magnetic field's configuration [*Liehmon et al.*, 2003]. In another way, this lack of relation between intensity of the emission and intensity of the incident energy flux may be simply due to fact that the measured ASPERA-3/ELS electron population is not representative of the precipitating population at the origin of the auroral emission. Several explanations are possible. For example, this is true if ASPERA-3/ELS' field of view did not cover the downward part of the electron distribution, if the electrons did not move radially between the spacecraft altitude and the Martian atmosphere, or if the electron distribution changed significantly from the spacecraft altitude to the Martian atmosphere (acceleration, backscattering. . .).

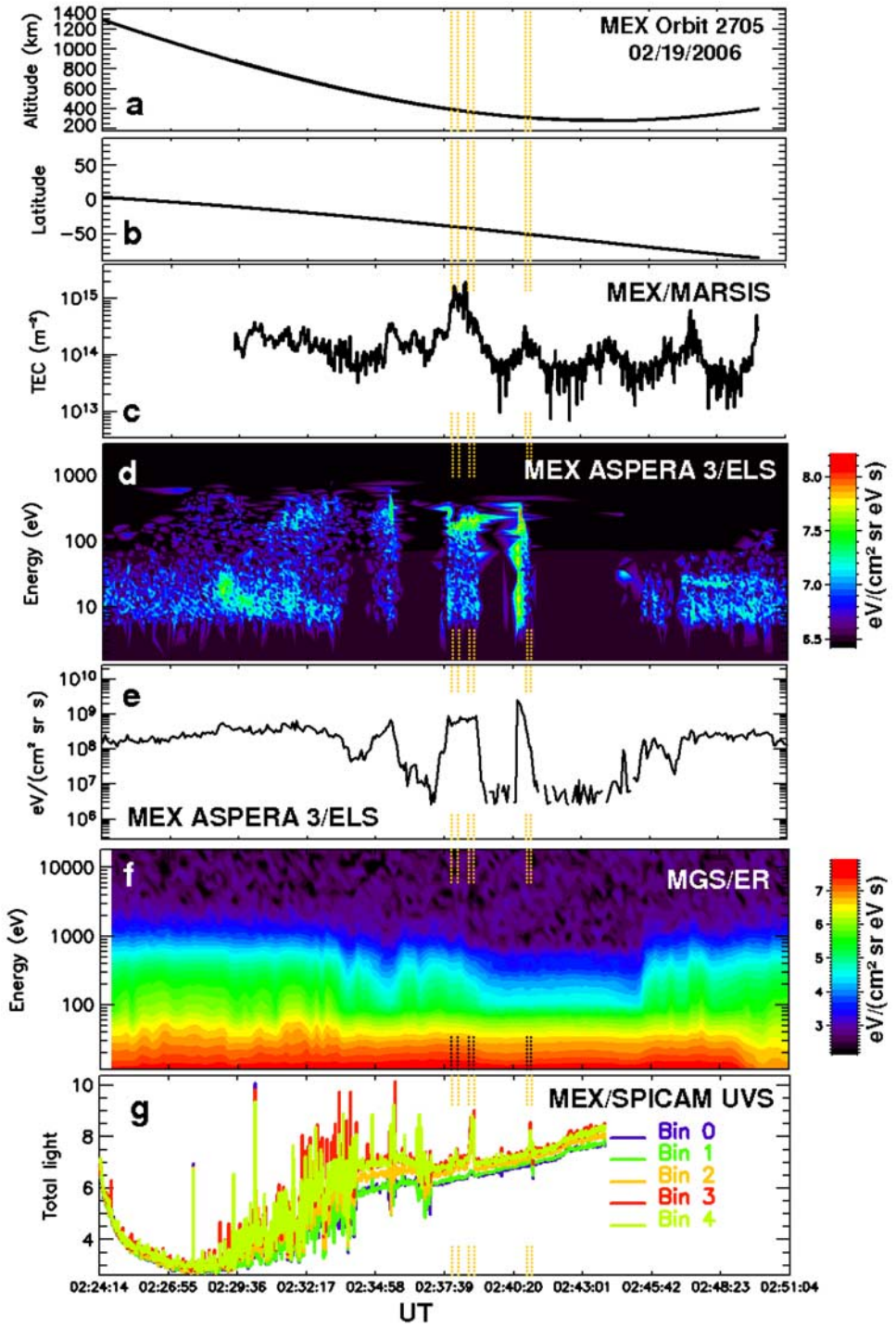


Figure 6. Time series of the measurements during orbit 2705. Shown is the MEX (a) altitude and (b) latitude, (c) MEX/MARSIS Total Electron Content, (d) MEX/ASPERA-3/ELS sector 1 (which is the sector facing the zenith) electron measurement in eV/(cm^2 ster eV s), (e) MEX/ASPERA-3/ELS energy flux of sector 1, (f) MGS/MAG-ER electron energy flux averaged over the full set of sectors in eV/(cm^2 ster eV s), and (g) MEX/SPICAM UVS measurements summed over the full spectral range for each spatial bin in ADU. Indicated on each panel by vertical dotted lines are the periods during which an aurora event has been identified in SPICAM UV observations.

[20] There is clearly, as shown in Figures 4 and 6, a high temporal correlation between the increase of the TEC as measured by MARSIS and the occurrence of an auroral event detected by SPICAM UVS. *Safaeinili et al.* [2007] have suggested that on the nightside, the observed peaks in the TECs with a high correlation with crustal magnetic field lines might indicate the local ionization of the Martian atmosphere where particles precipitate along these field lines. The convolution of

Table 2. Nadir Viewing Measured Aurora Events by SPICAM UVS/MEX[a]

Date MEX Orbit	Label	S/C Altitude (km)	Cameron Band Emission (R)	Emission at 289 nm (R)	Cameron Band/289 nm emissions	Electron Energy Flux 10^9 eV/(cm^2 sr s)	Peak in Energy (eV)	TEC Value (10^{15} m^{-2})
2004 07 07 591	591a	670	105 ± 10	N/A.	N/A.	4.2	∼350	N/A
	591b	586	195 ± 10	13 ± 8	15 ± 10	1.3	∼50	N/A
2005 12 27 2515	2515a	954	175 ± 16	50 ± 26	3.5 ± 2	4.1	∼190	N/A
	2515b	700	662 ± 24	120 ± 30	5.5 ± 1.6	7.8	∼150	0.27
2006 01 26 2621	2621a	564	274 ± 14	34 ± 15	8 ± 4	1.4	∼80	4.5
2006 02 19 2705	2705a	387	105 ± 9	27 ± 11	4 ± 2	2.2	∼160	11.6
	2705b	365	547 ± 16	94 ± 15	5.8 ± 1	2.3	∼200	3.8
	2705c	309	214 ± 11	12 ± 8	18 ± 13	0.4	∼40	0.9

[a]The Cameron band and 289 nm emissions are the values given in Table 1 for the lowest spectral resolution that is for the highest sensitivity of SPICAM UVS. The electron energy flux values are the integrated energy flux measured in sector 1 of ASPERA-3/ELS during the period of the aurora event. The peak of energy is the energy at which the electron flux distribution reached its maximum in sector 1. The TEC is the integrated total electron content during the period of the aurora event as measured by MARSIS. N/A indicates either that the emission was not estimated at better than one sigma uncertainty or that the TEC was not available because MARSIS was not deployed at that time or because MEX was too high in altitude.

the ionization cross sections of the main neutral species of the Martian atmosphere (essentially CO_2, the other species being minor) with the electron distribution measured by ASPERA-3/ELS therefore provide a first-order estimate of the total ionization rate induced by such an impacting flux. However, we did not find any evidence of a relation between measured TEC values and measured energy electron flux during the auroral events. As an example the largest TEC value from the 2705a event corresponds to a value of the electron energy flux close to the 2705b or 2621a events, whereas the measured TEC value is 3 times smaller during these two latter events. In contrast, the smallest TEC value (event 2515b) corresponds to the largest electron energy flux measured by ASPERA-3/ELS for this set of aurora events. This apparent lack of correlation between measured TEC and impacting electron fluxes may have three explanations. The first one is that the electrons measured by ASPERA-3/ELS did not precipitate directly below the S/C where the TEC is measured. The second explanation could be that there is no real direct relation between the ionization rate associated with the precipitating energy electron flux and the value of the atmospheric electron content. The third explanation is related to the difficulty in retrieving TEC values from the distortion in the MARSIS signal generated when the variation of the TEC is relatively short in time as in the cases of auroral events. Thus, *Mouginot et al.* [2008] estimated the nighttime mean sensitivity on a TEC determination as being equal to 1.5×10^{-14} m^{-2}, which is significantly large when compared to the values of the TEC given in Table 2, column 9.

[21] Another way to look for a potential link between ASPERA-3/ELS measurements and SPICAM UVS observations is to calculate the ratio, when available, between the measured intensity of the Cameron band emission and the intensity of the doublet at 289 nm. As explained by *Leblanc et al.* [2006b], this ratio is highly dependent on the energy of the precipitating electrons that may produce the observed emissions. Indeed the cross section of the production of the Cameron band emission peaks at an electron energy of around 80 eV, whereas the cross section for the production of the 289 nm doublet peaks at 150 eV [*LeClair and McConkey*, 1994]. In Table 2, column 7, we have calculated the ratios between the Cameron band emission and the 289 nm doublet emission. There is an evident relation between the large value of this ratio (between 8 and 18) and the electron distribution peaking below 80 eV (column 8), and between the small value of this ratio (between 3 and 6) and the electron distribution peaking above 150 eV. This result suggests that the particles at the origin of the measured emission probably have an energy distribution close to the energy distribution measured at higher altitudes, even if the energy flux intensity has probably changed from the altitude of ASPERA-3/ELS down to the regions of production of the observed glow.

3.4. Localization and Occurrence of UV Auroral Emissions

[22] Figure 7 is a zoom of the region where the aurora events have been observed by SPICAM UVS plotted on a map of the probability to be on a region of closed field lines at 400 km altitude as calculated by *Brain et al.* [2007]. This map has been built using 6 years of MGS/ER data set during the mapping orbit (between 1 July 1999 and 1 July 2005) on a nearly circular orbit of 405 ± 36 km at 0200/1400 local time. More than 20 million pitch angle electron distributions measured by MGS/ER on the nightside and in the energy channel 95–148 eV have been grouped into 27 different types of pitch angle distributions. In particular, regions with two-side loss cone electron distributions or no detection of electron flux (plasma voids region) have been considered regions of closed crustal magnetic field lines. The map displayed in Figure 7 is the probability to find such a type of distribution in MGS/ER data set with respect to planetary longitude and latitude. Similar maps for the open field line regions have also been built but are not used here because as explained by *Brain et al.* [2007], the association between electron pitch angle distributions and open field lines is more ambiguous. As shown in Figure 7, most of the auroral emissions identified by SPICAM UVS were detected in regions of local minimum of the probability to be on close field line regions, that is, in magnetic field regions that have cusp-like structure.

[23] *Lundin et al.* [2006] observed that the auroral-type electron energy distributions are usually observed at the boundary between open and closed field lines in good analogy with the Earth's auroral zone, so that auroral emission should preferentially occur at such a boundary. Auroral emissions should therefore be observed with a higher probability when the pass of the spacecraft crosses a boundary from closed to open field lines and vice versa. In some cases, we observed two consecutive and spatially close aurora events that may be associated to the passing of SPICAM UVS FOV over an open field line region bounded

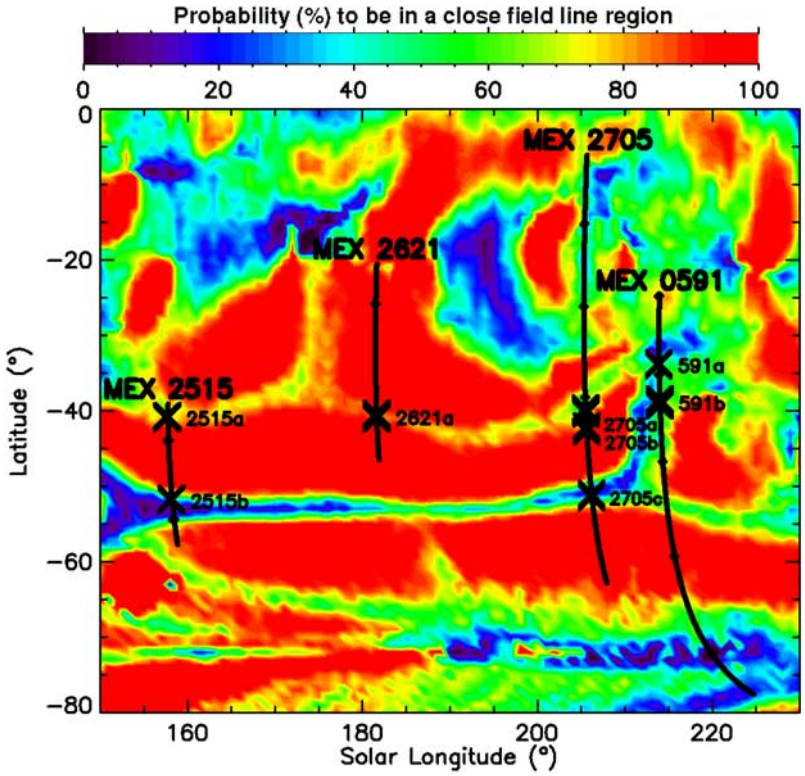


Figure 7. Map of the probability (expressed in percentage) to be in a closed field line region at 400 km in altitude on the Martian nightside as calculated from the Electron Reflectometer on board Mars Global Surveyor (MGS) during its mapping phase orbit. Electron pitch angle distributions have been recorded by the MGS magnetometer/electron reflectometer every 2 to 8 s during the spacecraft mapping orbit phase at around 400 km. Pitch angle distributions recorded in a single instrument energy channel (115 eV, a channel typically uncontaminated by photoelectrons) have been classified according to their shape. Also plotted are the trajectories of Mars Express (black line) below 1000 km altitude for the four orbits with aurora events. The crosses indicate the position of the aurora events identified in SPICAM UVS data. The spacecraft was moving from Northern to Southern Hemispheres.

by two closed crustal magnetic field line regions (e.g., passing into and out of a crustal cusp-like field structure). This may be what SPICAM UVS has observed in the case of orbit 2705 for events 2705a and 2705b (as also suggested by MARSIS measurements, Figure 6), and probably for the case of orbit 2621 as discussed previously (see Figure 4, MARSIS measurements) and the case of orbit 591 as shown in Figure 7. In cases 2515a, 2515b, and 2705c, no other auroral emission within ±20 s has been recorded even if Mars Express was above a large region of open field lines and relatively low in altitude (Figure 7). It may suggest that the current system was differently organized in these aurora regions. It may be also, as underlined by *Dubinin et al.* [2008b], that the map inferred from MGS/ER data obtained at a local time of 0200/1400 might be significantly different at a local time of 2030 (MEX local time during the considered orbits). As an example, *Dubinin et al.* [2008b] underlined the lack of any statistically significant enhancement of electron precipitation between latitude −50° and −55° in the same longitudinal range as measured by ASPERA-3/MEX, suggesting that the extended region of open field lines of Figure 7 might be significantly different at such a local time.

[24] On the other hand, as shown in Figure 3, several orbits occurred over the crustal magnetic field regions with no aurora event signature identified in SPICAM UVS data. Moreover, some of these orbits passed over regions where we positively identified an aurora event during previous or following orbits. As an example during orbit 2694, around 0031 UT, three days before orbit 2705, no aurora event was detected. Actually, precipitation of electrons into the Martian atmosphere has been shown by E. M. Dubinin et al. (Access of solar wind electrons into the Martian magnetosphere, submitted to *Annales Geophysicae*, 2008) and *Brain et al.* [2006] to depend strongly on the solar wind conditions. In particular, the interplanetary magnetic field orientation inducing a southward electric field direction should strongly favor the Southern Hemisphere access to the solar wind electrons (in good agreement with the dawnward direction of the IMF as inferred during orbit 2621 and 2705, see Table 1, column 4). During orbit 2694, the IMF, as determined half an hour before and 1 h after was close to a duskward direction (see http://sprg.ssl.berkeley.edu/∼brain/proxies/drapingdirxn.html). Such a dependency may explain the lack of auroral events observed during a MEX pass over the crustal magnetic field region but not the lack of consecutive events as discussed previously. Dubinin et al. (submitted manuscript, 2008) have built a map of the electron precipitation with energy spanning between 40 and 80 eV as measured by Mars Express/ASPERA-3/ELS between 250 and 600 km in altitude (Dubinin et al., submitted

manuscript, 2008, Figure 13c) in the highest crustal magnetic field regions. These authors have found that the largest flux of electrons occurred below −60° in latitude, whereas SPICAM UVS did not observe any auroral event below such latitude. Such an apparent discrepancy might be simply due to the poor statistic of SPICAM UVS detection.

4. Conclusions

[25] SPICAM UVS have identified several new auroral events for which it has been possible to obtain coordinated measurements with MARSIS and ASPERA-3/ELS. In order to avoid any ambiguity on the positions of the measurements, we used nadir configurations. This new set of observations shows quite strong coincidences between the occurrence of energetic precipitating electrons into the Martian atmosphere, the presence of crustal magnetic field anomalies and auroral-type glow. In some of these cases, there is a good probability that simultaneous measurements of the precipitating electron flux, of the induced UV aurora emission and of the produced total electronic content have been obtained leading to unprecedented information on the Martian aurora. Following the definition of *Brain et al.* [2007] of open/closed magnetic field lines, we observe that the few aurora detected by SPICAM UVS occur essentially in the region where the probability to be on closed field lines is small. Because the regions covered by SPICAM UVS are essentially where the crustal magnetic fields are present, we cannot firmly conclude on the role of crustal magnetic fields in triggering the Martian aurora. However, the positions of the identified aurorae in regions with the locally smallest probability to be on closed field lines suggests a significant relation between aurora events at Mars and the presence of cusp-like magnetic field line structures in good analogy with the Earth's auroral regions [*Lundin et al.*, 2006].

[26] **Acknowledgments.** Wolfgang Baumjohann thanks the reviewers for their assistance in evaluating this paper.

References

Acuña, M. H., et al. (2001), Magnetic field of Mars: Summary of results from the aerobraking and mapping orbits, *J. Geophys. Res.*, *106*, 23,403–23,417, doi:10.1029/2000JE001404.

Avakyan, S. V., et al. (1998), *Collision Processes and Excitation of UV Emission From Planetary Atmospheric Gases: A Handbook of Cross Sections*, Gordon and Breach, Amsterdam.

Barth, C. A., C. W. Hord, J. B. Pearce, K. K. Kelly, G. P. Anderson, and A. I. Stewart (1971), Mariner 6 and 7 Ultraviolet Spectrometer Experiment: Upper atmosphere data, *J. Geophys. Res.*, *76*, 2213–2227, doi:10.1029/JA076i010p02213.

Bertaux, J.-L., F. Leblanc, O. Witasse, E. Quémerais, J. Lilensten, A. S. Stern, B. Sandel, and O. Korablev (2005), Discovery of aurora on Mars, *Nature*, *435*, 790–794, doi:10.1038/nature03603.

Bertaux, J. L., et al. (2006), SPICAM on Mars Express: Observing modes and overview of UV spectrometer data and scientific results, *J. Geophys. Res.*, *111*, E10S90, doi:10.1029/2006JE002690.

Brain, D. A., J. S. Halekas, L. M. Peticolas, R. P. Lin, J. G. Luhmann, D. L. Mitchell, G. T. Delory, S. W. Bougher, M. H. Acuña, and H. Rème (2006), On the origin of aurorae on Mars, *Geophys. Res. Lett.*, *33*, L01201, doi:10.1029/2005GL024782.

Brain, D. A., R. J. Lillis, D. L. Mitchell, J. S. Halekas, and R. P. Lin (2007), Electron pitch angle distributions as indicators of magnetic field topology near Mars, *J. Geophys. Res.*, *112*, A09201, doi:10.1029/2007JA012435.

Cain, J. C., B. R. Ferguson, and D. Mozzoni (2003), An $n = 90$ internal potential function of the Martian crustal magnetic field, *J. Geophys. Res.*, *108*(E2), 5008, doi:10.1029/2000JE001487.

Carlsson, E., et al. (2006), Mass composition of the escape plasma at Mars, *Icarus*, *182*, 320–328, doi:10.1016/j.icarus.2005.09.020.

Chassefière, E., F. Leblanc, and B. Langlais (2006), The combined effects of escape and magnetic field histories at Mars, *Planet. Space Sci.*, *55*, 343–357, doi:10.1016/j.pss.2006.02.003.

Crider, D. H., D. Vignes, A. M. Krymskii, T. K. Breus, N. F. Ness, D. L. Mitchell, J. A. Slavin, and M. Acuña (2003), A proxy for determining solar wind dynamic pressure at Mars using Mars Global Surveyor data, *J. Geophys. Res.*, *108*(A12), 1461, doi:10.1029/2003JA009875.

Dubinin, E., G. Chanteur, M. Fraenz, and J. Woch (2008a), Field-aligned currents and parallel electric field potential drops at Mars: Scaling from the Earth's aurora, *Planet. Space Sci.*, *56*, 868–872.

Dubinin, E., M. Fraenz, J. Woch, J. D. Winningham, R. Frahm, R. Lundin, and S. Barabash (2008b), Suprathermal electron fluxes on the nightside of mars. ASPERA-3 observations, *Planet. Space Sci.*, *56*, 846–851.

Leblanc, F., J. Y. Chaufray, O. Witasse, J. Lilensten, and J.-L. Bertaux (2006a), The Martian dayglow as seen by SPICAM UV spectrometer on Mars Express, *J. Geophys. Res.*, *111*, E09S11, doi:10.1029/2005JE002664.

Leblanc, F., O. Witasse, J. Winningham, D. Brain, J. Lilensten, P.-L. Blelly, R. A. Frahm, J. S. Halekas, and J. L. Bertaux (2006b), Origins of the Martian aurora observed by Spectroscopy for Investigation of Characteristics of the Atmosphere of Mars (SPICAM) on board Mars Express, *J. Geophys. Res.*, *111*, A09313, doi:10.1029/2006JA011763.

LeClair, L. R., and J. W. McConkey (1994), (^{1}S) and CO($a^3\Pi$) production from electron impact dissociation of CO_2, *J. Phys. B At. Mol. Phys.*, *27*, 4039–4055.

Liehmon, M. W., D. L. Mitchell, A. F. Nagy, J. L. Fox, T. W. Reimer, and Y. Ma (2003), Comparisons of electron fluxes measured in the crustal fields at Mars by the MGS magnetometer/electron reflectometer instrument with a B field-dependent transport code, *J. Geophys. Res.*, *108*(E12), 5134, doi:10.1029/2003JE002158.

Liehmon, M. W., Y. Ma, A. F. Nagy, J. U. Kozyra, J. D. Winningham, R. A. Frahm, J. R. Sharber, S. Barabash, and R. Lundin (2007), Numerical modelling of the magnetic topology near Mars aurora observations, *Geophys. Res. Lett.*, *34*, L24202, doi:10.1029/2007GL031806.

Lundin, R., and S. Barabash (2004), Evolution of the Martian atmosphere and hydrosphere: Solar wind erosion studied by ASPERA-3 on Mars Express, *Planet. Space Sci.*, *52*, 1059–1071, doi:10.1016/j.pss.2004.07.020.

Lundin, R., et al. (2006), Plasma acceleration above Martian magnetic anomalies, *Science*, *311*, 980–983, doi:10.1126/science.1122071.

Mitchell, D. L., R. P. Lin, C. Mazelle, H. Réme, P. A. Cloutier, J. E. P. Connerney, M. H. Acuña, and N. F. Ness (2001), Probing Mars' crustal magnetic field and ionosphere with the MGS Electron Reflectometer, *J. Geophys. Res.*, *106*, 23,419–23,427, doi:10.1029/2000JE001435.

Mouginot, J., W. Kofman, A. Safaeinili, and A. Herique (2008), Correction of the ionospheric distortion on the MARSIS surface sounding echoes, *Planet. Space Sci.*, *56*, 917–926.

Nagy, A. F., et al. (2004), The plasma environment of Mars, *Space Sci. Rev.*, *111*, 33–114, doi:10.1023/B:SPAC.0000032718.47512.92.

Picardi, G., et al. (2004), Mars Express: A European mission to the red planet, *Eur. Space Agency Spec. Publ.*, *ESA SP 1240*, 51–70.

Purucker, M., D. Ravat, H. Frey, C. Voorhies, T. Sabaka, and M. Acuña (2000), An altitude-normalized magnetic map of Mars and its interpretation, *Geophys. Res. Lett.*, *27*, 2449–2452, doi:10.1029/2000GL000072.

Safaeinili, A., W. Kofman, J. Mouginot, Y. Gim, A. Herique, A. B. Ivanov, J. J. Plaut, and G. Picardi (2007), Estimation of the total electron content of the Martian ionosphere using radar sounder surface echoes, *Geophys. Res. Lett.*, *34*, L23204, doi:10.1029/2007GL032154.

Winningham, J. D., et al. (2006), Electron oscillations in the induced Martian magnetosphere, *Icarus*, *182*, 360–370.

J. L. Bertaux, Service d'Aéronomie, CNRS, IPSL, F-91371 Verrières-le-Buisson, France.

D. A. Brain and J. Halekas, Space Sciences Laboratory, University of California, Berkeley, CA 94720, USA.

R. A. Frahm and J. D. Winningham, Southwest Research Institute, San Antonio, TX 78228-0510, USA.

Y. Futaana, M. Holmström, R. Lundin, and H. Nilsson, Swedish Institute of Space Physics, Box 812, S-98 128, Kiruna, Sweden.

W. Kofman, J. Lilensten, and J. Mouginot, Laboratoire de Planétologie de Grenoble, F-38041 Grenoble CEDEX 9, France.

F. Leblanc, Osservatorio Astronomico di Trieste, Via Tieppolo 11, I-34131, Trieste, Italy. (francois.leblanc@aerov.jussieu.fr)

A. Safaenili, Jet Propulsion Laboratory, Pasadena, CA 91109, USA.

O. Witasse, Research and Scientific Support Department, ESA, ESTEC, NL-2200 AG Noordwijk, Netherlands.